Original article

In silico design of a multi-epitope vaccine targeting human immunodeficiency virus–tuberculosis co-infection: A reverse vaccinology approach to synergistic pathogenesis

Nabil Athoillah[a,*], Muhammad Irsyad Amien[a], Saski Yasmin Alfina[a], Ichlasul Mahdi Fardhani[a], Irsyad Lutfi Elfahmi[a], Putri Ayu Ardiani[a], Mukhammad Arif Hadi Khoiruddin[a], Mohammad Alifi Agfareza[b], Mitsla Chusnica Aulia As'ar[c], Angga Mardro Raharjo[d], Atika Purnama Sari[e]

[a]*Faculty of Medicine, University of Jember, Jember, Indonesia*
[b]*Faculty of Medicine, University of Gadjah Mada, Yogyakarta, Indonesia*
[c]*Faculty of Medicine, University of Papua, Sorong, Indonesia*
[d]*Department of Pulmonology and Respiratory Medicine, Faculty of Medicine, University of Jember, Jember, Indonesia*
[e]*Department of Internal Medicine, Faculty of Medicine, University of Jember, Jember, Indonesia*

Proof Version

Abstract

Background: The synergism between *Mycobacterium tuberculosis* (Mtb) and human immunodeficiency virus (HIV) represents a global health crisis, where co-infection significantly accelerates immune failure and exacerbates mortality rates.

Objective: This study aimed to design *in silico* a novel multi-epitope vaccine predicted to stimulate robust, long-lasting, and concurrent immune protection against Mtb and HIV.

Methods: This reverse vaccinology study followed a multi-level immunoinformatic approach. We predicted cytotoxic T lymphocyte (CTL), helper T lymphocyte (HTL), and linear B-cell (LBL) epitopes. Each was tested for its ability to induce an immune response without evoking allergic or toxic reactions. Select epitopes were combined into a multi-epitope vaccine construct bearing adjuvants and linkers. It was analyzed for physicochemical characteristics, solubility, structural modeling, molecular docking with toll-like receptor 4 (TLR 4), and stability. Immune simulations, codon optimization, and *in silico* cloning helped assess immunogenicity and establish expression potential.

Results: Proteomics prioritized 23 epitopes—11 CTL, 5 HTL, and 7 LBL. Each demonstrated high antigenicity, non-allergenicity, and non-toxicity. The final vaccine construct exhibited superior stability in normal mode analysis and strong binding affinity for TLR4, as evidenced by low-energy docking scores. Immune simulations predicted a robust secondary immune response, characterized by significant increases in antibody titers, B-cell memory, and the release of Th1-polarized cytokines: IFN-gamma and interleukin-2. The global HLA population coverage was estimated at 99.3%, indicating broad-spectrum protective potential.

Conclusion: The multi-epitope vaccine designed here exhibited high predicted stability, safety, and robust *in silico* immunogenic potential. Overall, this construct is a promising candidate for a unified preventive strategy against HIV−TB co-infection, warranting further experimental validation in pre-clinical settings.

Keywords: Co-infection, human immunodeficiency virus, immunoinformatics, multi-epitope vaccine, tuberculosis.

Despite the widespread implementation of antiretroviral therapy (ART) and the Bacillus Calmette-Guérin (BCG) vaccine, the syndemic convergence of tuberculosis (TB) and the human immunodeficiency virus (HIV) remains one of the most formidable challenges to global public health. [1, 2] In individuals co-infected with HIV, the natural history of TB is profoundly altered; HIV-induced depletion of CD4+ T cells and an impairment of macrophage function significantly increase susceptibility to both primary *Mycobacterium tuberculosis* (Mtb) infection and reactivation of latent TB. [3] Conversely, Mtb triggers chronic immune system activation and systemic inflammation. The latter creates a cellular environment ideal for massive HIV replication. [4]

[*]**Correspondence to**: **Nabil Athoillah,** Faculty of Medicine, University of Jember, Jember, Indonesia.
E-mail: kaknabil2007@gmail.com
Received: May 30, 2026
Revised: July 10, 2026
Accepted: August 20, 2026

Open Access 2027 Athoillah et al., published by Faculty of Medicine, Chulalongkorn University. This work is licensed under the Creative Commons Attribution 4.0 International License.

The bidirectional interaction between TB and HIV markedly worsens prognosis.

Addressing HIV–TB co-infection requires a holistic strategy that integrates ART with robust tuberculosis treatment. While current ART protocols can achieve effective viral suppression, they fail to fully reconstitute TB-specific immune defenses within the respiratory mucosa, leaving patients extremely vulnerable to TB-associated mortality. [4, 5] Furthermore, the clinical management of HIV–TB co-infection is continuously hindered by complex drug–drug interactions, overlapping hepatotoxicity, and increasing emergence of multidrug-resistant TB (MDR-TB) strains. [6, 7] Such a dual burden underscores a critical, unmet clinical need for integrated preventive strategies. However, single-pathogen candidate vaccines existing within the clinical pipeline are not engineered to address the overlapping and synergistic immune exhaustion mechanisms unique to the HIV–TB syndemic. Therefore, developing a chimeric, dual-antigen vaccine that can simultaneously elicit robust and durable cell-level immunity against both pathogens is urgent. [8–10]

Rational design of such complex multivalent vaccines *via* conventional empirical methods is extremely challenging due to extensive genome sizes and high mutation rates of these pathogens, particularly HIV-1. In this context, *in silico* immunoinformatics and reverse vaccinology offer a transformative approach. Utilizing computational algorithms and structural modeling, these tools enable precise identification of highly immunogenic, non-allergenic T- and B-cell epitopes derived from essential virulence factors based on large-scale proteomic data, allowing rapid, accurate construction of multi-epitope assemblies. [11, 12] While computational studies have successfully proposed multi-epitope vaccines against either Mtb or HIV individually, an integrated chimeric vaccine targeting the specific immunological intersections of the two pathogens remains largely unexplored.

To bridge such a significant research gap, this study aimed to computationally engineer a novel, dual-antigen multi-epitope subunit vaccine against HIV–TB co-infection. By targeting literature-validated virulence factors essential for mycobacterial intracellular survival and viral immune evasion and computationally evaluating the structural dynamics of vaccine–receptor interactions through normal mode analysis (NMA), this study proposes a theoretically stable and potentially immunogenic candidate for subsequent pre-clinical evaluation.

Materials and methods

Protein sequence retrieval and immunogen selection

The initial phase involved retrieving high-priority protein sequences from both *M. tuberculosis* and HIV-1. Virulence factors and essential proteins were identified by accessing the Virulence Factor Database (VFDB; https://www.mgc.ac.cn/VFs/) and the Bacterial and Viral Bioinformatics Resource Center (BV-BRC; https://www.bv-brc.org/), and corroborated them with literature on synergistic pathogenesis. [13,14] To ensure safety and prevent molecular mimicry, sequences with high homology to the human proteome were excluded. [15] For Mtb, Ag85, ESX-1/EccB, plcA/B/C, EIS, SapM, eccCa1, and eccCb1 were selected due to their pivotal roles in early host cell invasion and intracellular survival within macrophages. [16,17] For HIV, Vif, Nef, Vpr, and gp120 were chosen as they actively downregulate host major histocompatibility complex (MHC) molecules and induce T-cell apoptosis, directly exacerbating mycobacterial co-infection.

Human proteome cross-reactivity

We systematically searched each prioritized candidate epitope and the final construct for homology to human proteins to eliminate the risk of molecular mimicry and vaccine-induced autoimmunity. Cross-reactivity was examined utilizing the NCBI BLASTp (Basic Local Alignment Search Tool) algorithm against the non-redundant (nr) protein database, restricted to the *Homo sapiens* reference proteome (TaxID: 9606). Alignment criteria were established *a priori* to define significant homology. Any epitope or region with i) $P < 0.05$, ii) sequence identity of $\geq 35.0\%$, and iii) query coverage of $> 70.0\%$ with any human protein was considered potentially cross-reactive and excluded.

CTL and HTL epitope prediction

Cytotoxic T lymphocyte (CTL) 10-mer epitopes were predicted employing the NetMHCpan 4.1 EL algorithm via the IEDB MHC-I tool (http://tools.iedb.org/mhci/) to ensure robust binding profiles across diverse populations. The two classes were cross-validated; CTL epitopes were selected at a high-affinity percentile rank cutoff of ≤ 0.2. Binding affinities were assessed against a set of prevalent HLA class I alleles. The reference panel of HLA alleles was selectively curated to represent the greatest allelic frequencies in regions with the heaviest HIV–TB syndemic burden (e.g., East Asia and Sub-Saharan Africa), ensuring

Proof Version

downstream clinical relevance. [18] Similarly, 15-mer helper T lymphocyte (HTL) epitopes were identified using the NetMHCIIpan 4.1 EL method (http://tools.iedb.org/mhcii/). They were prioritized based on a percentile rank cutoff of ≤ 2.0. [19] CTL and HTL epitopes were selected based on percentile ranks and IC_{50} values to ensure robust $CD8^+$ and $CD4^+$ T-cell activation.

Linear B-cell epitope prediction

Linear B-cell epitopes, ranging from 12 to 16 residues, were predicted utilizing the Bepipred Linear Epitope Prediction tool (http://tools.iedb.org/bcell/). [19] Selection criteria focused on residue flexibility and surface accessibility, crucial determinants of antibody-mediated recognition of B-cell receptors.

Assessment of antigenicity, allergenicity, and toxicity

The application potential of each predicted epitope as a vaccine was screened rigorously. As a primary filtering mechanism, sequence-based predictions were applied to individual epitopes before full assembly. Antigenicity was ascertained employing the VaxiJen v2.0 server with a threshold of ≥ 0.4. [20] Potential allergenicity was evaluated utilizing the AllerTOP v2.0 server and auto-cross covariance transformation. [21] Toxicity profiles of the shortlisted peptides were assessed in ToxinPred, which employs machine learning to evaluate sequence-based physicochemical parameters, ensuring safety. [22] An antigenicity threshold of ≥ 0.4 was strictly applied. However, single HTL epitopes demonstrating exceptional MHC-II binding affinity and critical multi-cytokine (e.g., interleukin (IL)-4/IL-10) induction capabilities were methodologically excluded, as their primary role is T-helper polarization rather than direct physicochemical antigenicity.

Immunogenicity and cytokine-inducing potential

CTL epitopes were analyzed for their capacity to elicit CD8z T-cell responses employing the IEDB immunogenicity tool. [19] For HTL epitopes, the IFNepitope server was utilized to identify interferon gamma (IFN-γ) inducers; IL4pred and IL10pred screened IL-4 and IL-10 inducers, respectively, to ensure a balanced pro-inflammatory and regulatory immune profile.[23, 24]

Population coverage analysis

The IEDB Population Coverage tool was employed to calculate the combined global and regional HLA coverage for the selected CTL and HTL epitopes. [19] This analysis ensured the vaccine's applicability across diverse ethnic groups, particularly in regions with an elevated burden of HIV–TB co-infection.

Design of the multi-epitope vaccine construct

Rather than segregating antigens, the selected TB and HIV epitopes were consecutively woven based on their predicted proteasomal cleavage patterns to prevent antigenic competition and facilitate simultaneous multi-pathogen presentation. Their structural integrity and functional presentation were optimized using well-characterized, sequence-specific linkers. [25] AAY linkers were inserted between CTL epitopes to enhance proteasomal cleavage and MHC-I presentation. "GPGPG" linkers were inserted between HTL epitopes to induce rigid β-turns to prevent junctional neo-epitope formation; KK spacers were used to separate LBL. [26] To augment mucosal immunogenicity, the Cholera Toxin B (CTB) subunit was selected as a molecular adjuvant and fused to the N-terminus. CTB is extremely effective at breaking mucosal tolerance, making it an ideal choice for combating respiratory (Mtb) and mucosal (HIV) pathogens. A rigid "EAAAK" linker was inserted between the CTB adjuvant and main antigenic sequence to ensure structural separation and prevent steric hindrance during receptor binding. [27]

Structural characterization and validation

Comprehensive three-dimensional (3D) structural analyses rather than linear 1D metrics established the viability of the fully assembled chimeric construct. Physicochemical properties, including the instability index and GRAVY score, were evaluated in ProtParam. [28] Secondary and tertiary structures were predicted in PSIPRED v4.0 and AlphaFold Server.[29,30] Structural refinement was conducted in GalaxyRefine and validated through Ramachandran plots in PROCHECK and Z-score assessment in ProSA-web. [31–33]

Molecular docking and normal mode

Toll-like receptor 4 (TLR4) was strategically selected as the target innate immune receptor due to its established dual-sensor role in the HIV–TB syndemic, recognizes mycobacterial virulence factors to initiate macrophage phagocytosis, and co-interacts with the HIV-1 envelope glycoprotein (gp120) to modulate downstream inflammatory signaling. [29] Before docking, the human TLR4 receptor crystal structure (PDB ID: 4G8A) was prepared in PyMOL; specifically, the functional monomer (chain A) was isolated, while all water molecules, heteroatoms, and

Proof Version

co-crystallized native ligands were strictly removed to expose the reactive interface. The vaccine construct and TLR4 receptor were molecularly docked using the ClusPro 2.0 server in a balanced mode to predict the relative binding conformation. To map the binding footprint post-docking, interface-associated residues and non-covalent interaction types (e.g., hydrogen bonds and electrostatic interactions) were visualized and extracted in PyMOL. [34] The stability and deformability of the vaccine–TLR4 complex were further analyzed through NMA in the iMODS server to evaluate collective functional motions. [35]

In silico immune simulation and cloning

Immune response-related dynamics were simulated *via* a three-dose immunization schedule in the C-ImmSim server. [36] Finally, to ensure heterologous expression, the vaccine sequence was codon-optimized for *Escherichia coli* (K12) using the JCat server. The optimized gene was then *in silico* cloned into the pET-30a(+) vector utilizing SnapGene. [37]

Ethical considerations

Regarding the IRB number, this study does not require IRB or ethical approval because it is an entirely *in silico* and bioinformatics-based study. The research does not involve human participants, animals, or the collection of human/animal biological samples or clinical data. Therefore, an IRB number is not applicable to this study.

Results

Prediction of T-cell epitopes and prioritization

In this study, a systematic computational pipeline identified high-affinity T-cell epitopes from Mtb virulence factors (Ag85, ESX-1/EccB, plcA/B/C, EIS, SapM, eccCa1, and eccCb1) and HIV-1 proteins (Vif, Nef, Vpr, and Gp120). CTL epitopes were predicted utilizing the IEDB MHC-I processing tool; HTL epitopes were screened by accessing the IEDB MHC-II binding prediction server. The initial CTL prediction generated 95,391 raw peptides. MHC-I affinity filtering excluded 95,142 non-binders, retaining 249 candidates. Subsequent screening for biosafety (non-allergenic, non-toxic) and baseline immunogenicity retained 34 safe epitopes. To optimize construct length and prevent antigenic competition, 11 candidates with maximum antigenicity scores were selected. The initial pool of 34,807 HTL peptides was filtered for MHC-II binding, yielding 664 binders. Subsequent biosafety screening and strict cytokine profiling (IFN-γ, IL-4, and IL-10 induction) narrowed this to 15 candidates, from which the top 5 were included to maintain construct stability and prevent steric hindrance. CTL and HTL epitope profiles are detailed in **Supplementary Tables S1-S2**, respectively.

B-cell epitope prediction and prioritization

LBL epitopes were predicted utilizing the Bepipred Linear Epitope Prediction 2.0 algorithm *via* the IEDB server. Initially, 58 potential LBL epitopes were predicted; all met the baseline structural thresholds—flexibility and surface accessibility. Next, 42 candidates were excluded following rigorous downstream screening for biosafety and functional potency—VaxiJen score ≥ 0.4, non-allergenic *via* AllerTOP, and non-toxic *via* ToxinPred. Of the remaining 16 high-quality candidates, the top 7 with maximum antigenicity scores were integrated into the multi-epitope construct. Comprehensive characteristics of the finalized LBL are presented in **Supplementary Table S3**.

Cross-reactivity between the designed vaccine candidate and human proteome

Safety profiles of the selected epitope sequences and the assembled multi-epitope construct were established against the *Homo sapiens* reference proteome using NCBI BLASTp. The search engine returned a strict "No significant similarity found" output. Consequently, zero sequence alignments met or exceeded our predefined exclusion thresholds. These results confirm that, at the sequence level, the selected epitopes were unique to the pathogen-derived targets and were extremely unlikely to induce cross-reactive autoimmune responses in host tissues. These results suggest that, at the sequence similarity level, the selected epitopes are unlikely to overlap with known human protein sequences. However, this analysis is limited to computational homology assessment and does not account for potential structural or conformational similarities. Within these constraints, the findings provide initial support for the specificity of selected epitopes toward pathogen-derived targets.

Evaluation of the antigenicity, allergenicity, and toxicity of the epitope vaccine candidate

Before assembling the final construct, individual CTL, HTL, and LBL epitopes were predicted for antigenicity, allergenicity, and toxicity to ensure immune suitability. Antigenicity prediction indicated that most selected epitopes met the applied VaxiJen threshold

Proof Version

criteria (score ≥ 0.4), with one HTL epitope from Ag85 (LLDGLRAQDDFSGWD) scoring 0.0277. However, it was strategically retained in the final construct, justified by its exceptionally robust MHC-II binding profile and its critical capacity to induce both IL-4 and IL-10, vital for establishing a balanced Th1/Th2 immune response within the global multi-epitope assembly. Furthermore, AllerTOP v.2.0 classified all prioritized epitopes as non-allergenic, and ToxinPred did not identify any toxic peptide features among the selected sequences.

Evaluation of CTL immunogenicity and HTL-induced IFN-γ, IL-4, and IL-10

The construct's potential to support cell-level immune activation was assessed by predicting CTL immunogenicity and cytokine induction by HTL epitopes. Immunogenicity prediction suggested that the included CTL epitopes can be recognized by CD8z T cells, indicating their suitability for inclusion in a cytotoxic T cell-oriented vaccine design. The selected HTL epitopes were predicted to induce IFN-γ, IL-4, and IL-10, suggesting their involvement in cellular, humoral, and regulatory immune pathways. Nevertheless, these findings are computational and require experimental validation to confirm the magnitude and balance of cytokine production.

Multi-epitope subunit vaccine construction

A multi-epitope subunit vaccine was obtained by assembling 11 CTLs, 5 HTLs, and 7 LBLs, concatenated with specific linkers: AAY, GPGPG, and KK, respectively **(Figure 1)**. A CTB subunit was fused to the N-terminus *via* an EAAAK linker. The final assembled construct comprised exactly 466 amino acid residues.

Proof Version

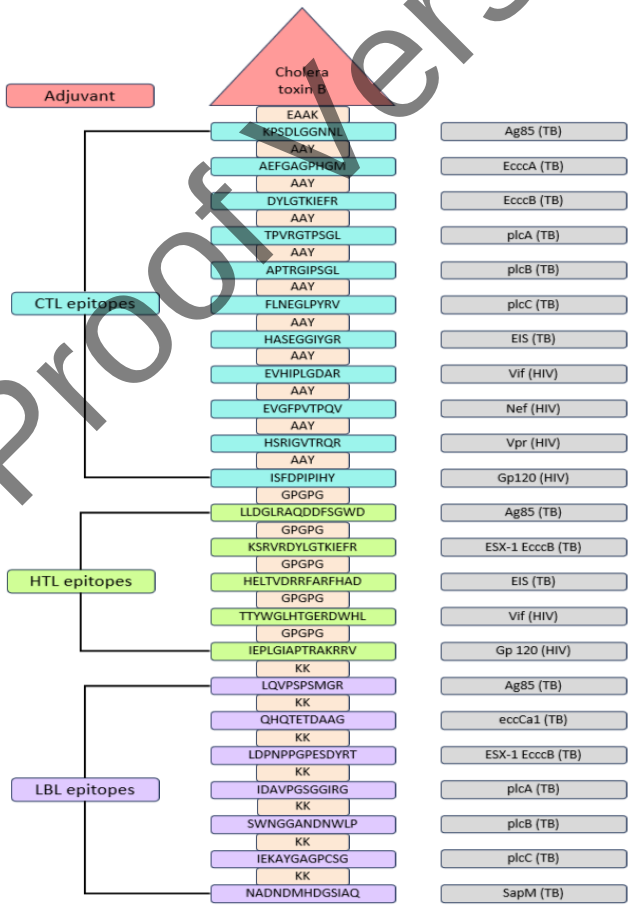


Figure 1. Schematic representation of the designed HIV-TB chimeric multi-epitope vaccine construct. The final 466-amino-acid construct consists of a Cholera Toxin B subunit as the N-terminal mucosal adjuvant, linked to the main antigenic sequence via a rigid EAAAK linker. The sequence incorporates 11 CTL, 5 HTL, and 7 LBL epitopes. To ensure optimal processing and prevent junctional neo-epitopes, the epitopes are interwoven using sequence-specific linkers: AAY for CTL, GPGPG for HTL, and KK for LBL epitopes. CTL, cytotoxic T lymphocyte; HTL, helper T lymphocyte; LBL, linear B cell.

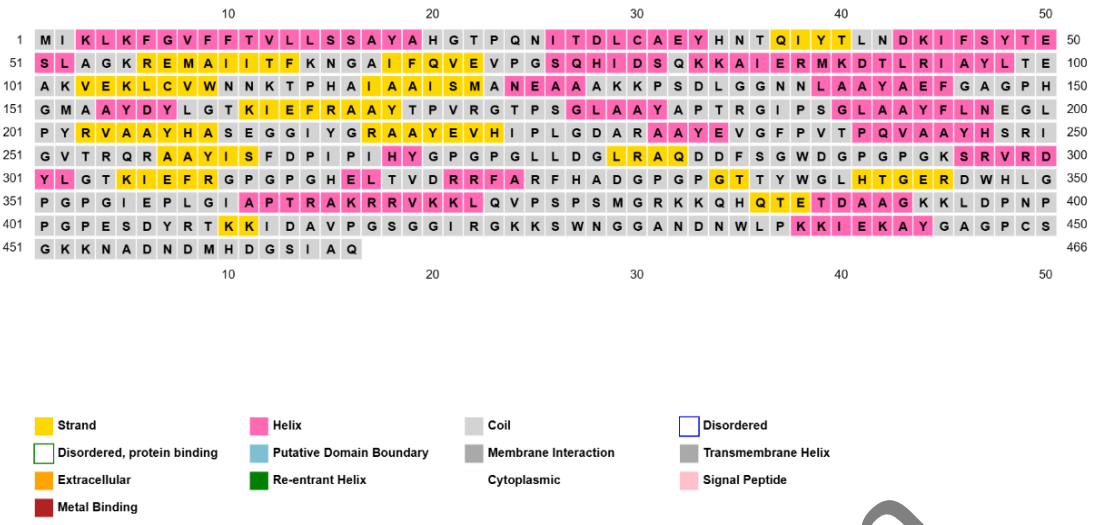


Figure 2. Predicted secondary structure of the HIV-TB multi-epitope vaccine construct. The structural distribution across the 466-amino acid sequence was predicted using PSIPRED. The graphical output illustrates a composition dominated by random coils (48.7%), followed by α-helices (33.26%), and β-strands (18.0%).

Table 1. Physichochemicalproperties analysis of our multi-epitope vaccine candidate.

Parameter	Value
Number of amino acids	466
Theoretical pI	9.34
Molecular weight	50360.96
Formula	C2255H3484N640O655
Total number of atoms	7044
Instability index	33.44
Estimated half-life:	30 hours (mammalian reticulocytes, *in vitro*) >20 hours (yeast, *in vivo*) >10 hours (*E. coli*, *in vivo*)
Aliphatic index	68.82
Grand average of hydropathicity (GRAVY)	-0.498

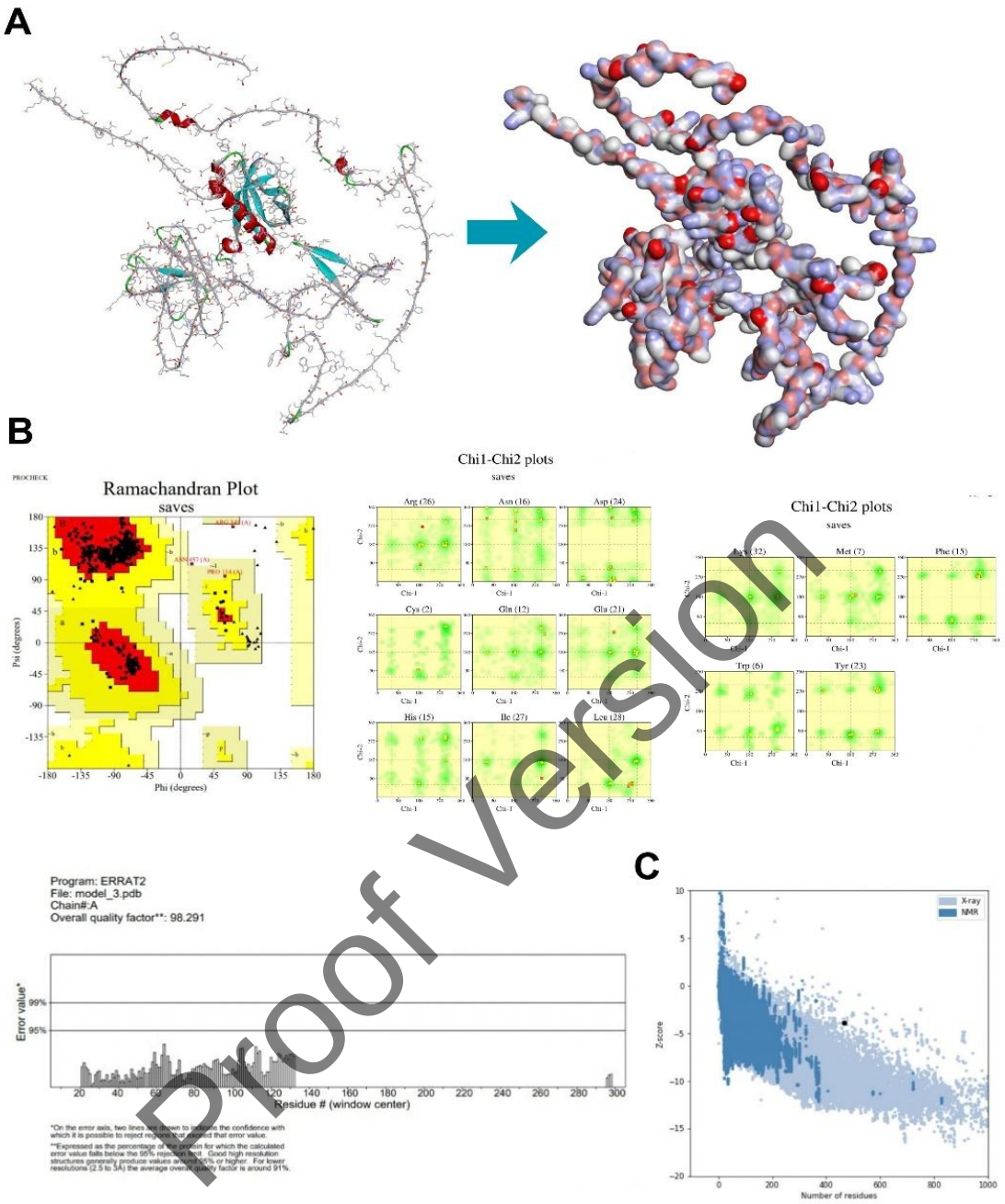
Proof Version

Secondary structure prediction

Secondary structure prediction of the finalized MEV construct evaluated its conformational characteristics and structural stability. As shown in **Figure 2**, it was predominantly composed of random coils: 48.7% (227), α-helices: 33.3% (155), and β-strands: 18.0% (84 residues). Physicochemical analysis quantified the molecular weight to be 50.36 kDa and the theoretical pI to be 9.34, indicating a basic protein. The instability index was calculated as 33.44, classifying the protein as stable. The estimated half-life was 30 h in mammalian reticulocytes (*in vitro*), over 20 h in yeast (*in vivo*), and over 10 h in *E. coli* (*in vivo*). Additionally, the aliphatic index was 68.82, suggesting moderate thermal stability, while the negative GRAVY value (−0.498) indicated hydrophilicity**(Table 1)**.

Tertiary structure modeling, refinement, and validation

The vaccine tertiary structure was modeled in the AlphaFold Server. The unrefined model generated exhibited a predicted template modeling (pTM) score of 0.30 and an overall average pLDDT score of 70.0. The N-terminal mucosal adjuvant (CTB) domain folded with high confidence, supported by a low predicted aligned error, indicating enhanced positional certainty. In contrast, the AlphaFold algorithm explicitly computed a fraction disordered score of 0.79, confirming that 79.0% of the construct (comprising the downstream concatenated epitope region) lacked a rigid tertiary structure. Such extensive structural fluidity is an expected and extremely favorable characteristic for multi-epitope chimeras. It correlates perfectly with our secondary structure predictions



Proof Version

Figure 3. Predicted 3D structure of the multi-epitope vaccine and its spatial validation. **(A)** The refined 3D tertiary structure modeled using AlphaFold, illustrating the spatial arrangement of the CTB adjuvant (in blue) and the concatenated epitope regions, **(B)** Ramachandran plot analysis (PROCHECK) of the refined model (94, 9.0%) and ERRAT Analysis (98, 2.0%), demonstrating that the vast majority of residues are located in the most favored regions, indicating high stereochemical quality and high resolution, **(C)** ProSA-web overall model quality analysis, displaying a Z-score of -3.84, which falls within the characteristic range of native proteins of similar size. CTB, Cholera toxin B.

(dominated by random coils) and theoretically facilitates downstream proteasomal degradation and optimal MHC presentation by antigen-presenting cells without severe steric hindrance. The structure was refined *via* GalaxyRefine (**Figure 3**). Structural validation using the ERRAT program yielded an overall quality factor of 98.29, indicating a high-quality model within the acceptable range for proteins of comparable size. Ramachandran plots with PROCHECK localized 94.9% (353) of amino acid residues within most favored regions, 4.6% (17) in additionally allowed regions, and only 0.5% (2) in disallowed regions. Further validation using the ProSA-web server produced a Z-score of −3.84, which falls within the range for experimentally determined proteins of similar length. In addition, side-chain stereochemistry assessment through Chi1–Chi2 plots demonstrated that most residues, including Asp, Glu, Ile, Leu, Lys, Met, and Phe, were distributed within preferred torsional regions, with only minor acceptable deviations.

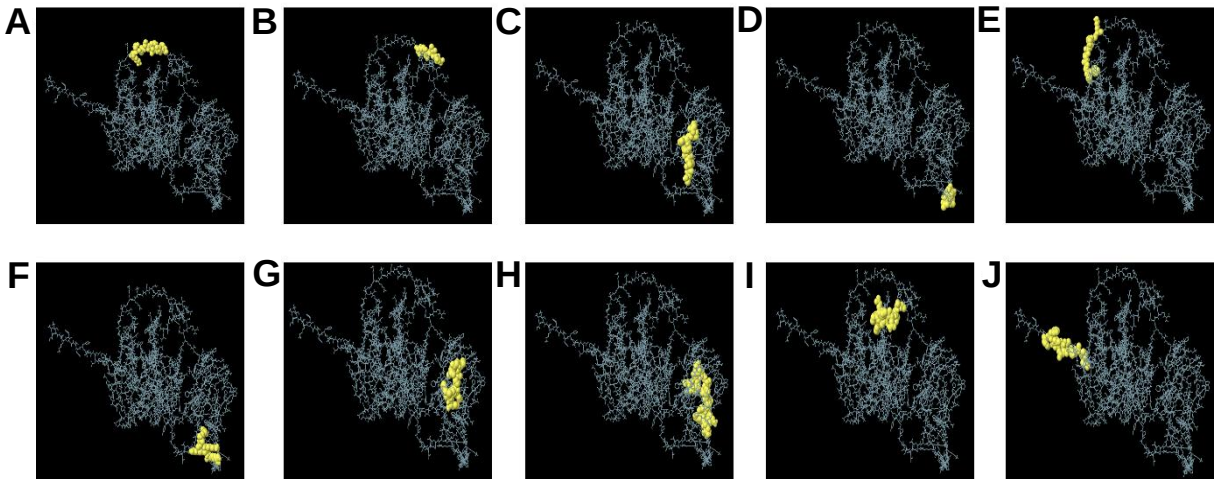


Figure 4. A total of 10 discontinuous B cell epitopes were identified in Ellipro which are exceeding the threshold Protrusion Index (PI) score of 0.7. The epitopes varied in length, ranging from 5 to 23 residues.

Conformational B-cell epitope identification of the final vaccine

In total, ten discontinuous LBL epitopes were identified using ElliPro, each exceeding the threshold protrusion index (PI) score of 0.7. The epitopes varied in length, from 5–23 residues. **Figure 4** lists the start and end positions of each epitope within the complete sequence, which were A:K453, A:N454, A:A455, A:D456, A:N457, A:D458, A:M459, A:H460 residues with 0.97 of PI score (**Figure 4A**); A:D461, A:G462, A:S463, A:I464, A:A465, A:Q466 residues with 0.97 of PI score (**Figure 4B**); A:E356, A:P357, A:L358, A:G359, A:I360, A:A361, A:P362, A:T363 residues with 0.89 of PI score (**Figure 4C**); A:L372, A:Q373, A:V374, A:P375, A:S376, A:P377, A:S378, A:M379, A:G380, A:R381 residues with 0.87 of PI score (**Figure 4D**); A:A443, A:Y444, A:G445, A:A446, A:G447, A:P448, A:C449, A:S450, A:G451, A:K452 residues with 0.86 of PI score (**Figure 4E**); A:R364, A:A365, A:K366, A:R367, A:R368 residues with 0.86 of PI score (**Figure 4F**); A:D346, A:W347, A:H348, A:L349, A:G350, A:P351, A:G352, A:P353, A:G354, A:I355 residues with 0.79 of PI score (**Figure 4G**); A:H385, A:Q386, A:T387, A:E388, A:T389, A:D390, A:A391, A:A392, A:G393, A:K394, A:K395, A:L396, A:D397, A:P398, A:N399, A:P400, A:P401, A:G402, A:P403, A:E404, A:S405, A:D406, A:Y407 residues with 0.79 of PI score (**Figure 4H**); A:E234, A:V235, A:G236, A:F237, A:P238, A:V239, A:T240, A:P241, A:Q242, A:V243, A:A244, A:A245 residues with 0.76 of PI score (**Figure 4I**); A:F9, A:F10, A:T11, A:V12, A:L13, A:L14, A:S15, A:S16, A:A17, A:Y18, A:A19 residues with PI score of 0.74 (**Figure 4J**).

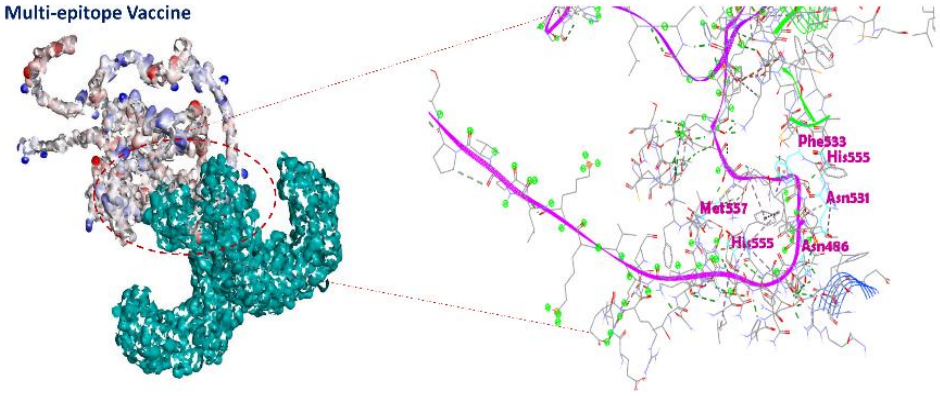
Molecular docking analysis and interaction studies

Vaccine–TLR4 receptor (chain A) binding affinity was evaluated through molecular docking simulations using the balanced mode of the ClusPro 2.0 server. Based on the coefficient weight analysis E = 0.40Erep ± 0.40Eatt + 600Eelec + 1.00EDARS, Cluster 0 was identified as the most representative. It comprised 73 members; the weighted score for the central pose was –1478.5, while the lowest energy reached –1725.5 **(Figure 5)**. These values represent the predictive thermodynamic probability of a favorable interaction. Detailed analysis of the docked complex interface revealed specific intermolecular associations driving this stability. The binding was stabilized by a network of hydrogen bonds between the vaccine and critical TLR4 binding pocket residues, notably Phe533, His555, Met557, Asn486, and Asn531 **(Figure 5)**. These predictive mappings suggest that the chimeric vaccine could structurally engage the TLR4 receptor, fulfilling the prerequisite for potential downstream innate immune responses.

Normal mode analysis

Structural stability, conformational flexibility, and biophysical properties of the vaccine–receptor complex were assessed through NMA in the iMODS server. The deformability plot exhibited multiple fluctuations, representing inherent vaccine flexibility during interaction with TLR4 **(Figure 6A)**. The NMA-calculated B-factor remained relatively consistent throughout the simulation, with only one minor fluctuation **(Figure 6B)**. The eigenvalue of 1.730773 $x10^{-7}$ suggests that a low-frequency flexible force is required for deformation, reflecting a favorable conformational stability of the complex **(Figure 6C)**.

Proof Version



Coefficient Weights

$$E = 0.40E_{rep} + -0.40E_{att} + 600E_{elec} + 1.00E_{DARS}$$

Cluster	Members	Representative	Weighted Score
0	73	Center	-1478.5
		Lowest Energy	-1725.5

Figure 5. Molecular docking interaction between the HIV-TB multi-epitope vaccine and the human TLR4 receptor. **(A)** The lowest-energy docked complex predicted by the ClusPro 2.0 server. The TLR4 receptor (Chain A) is depicted in green, and the vaccine construct is shown in grey and **(B)** A close-up, magnified view of the interaction interface, explicitly mapping the network of non-covalent interactions. Key interacting residues within the TLR4 binding pocket (including Phe533, His555, Met557, Asn486, and Asn531) and the corresponding hydrogen bonds (indicated by dashed lines) are highlighted, suggesting a favorable structural conformation for receptor engagement. TLR4, toll-like receptor 4.

Homogeneity was observed in the complex's conformational variance **(Figure 6D)**. The covariance matrix highlighted dominant coordinated rotational motions (indicated in red), suggesting stable collective residue movements during binding **(Figure 6E)**. Furthermore, the elastic network results confirmed a direct proportionality with the binding elasticity **(Figure 6F)**.

Immune simulation

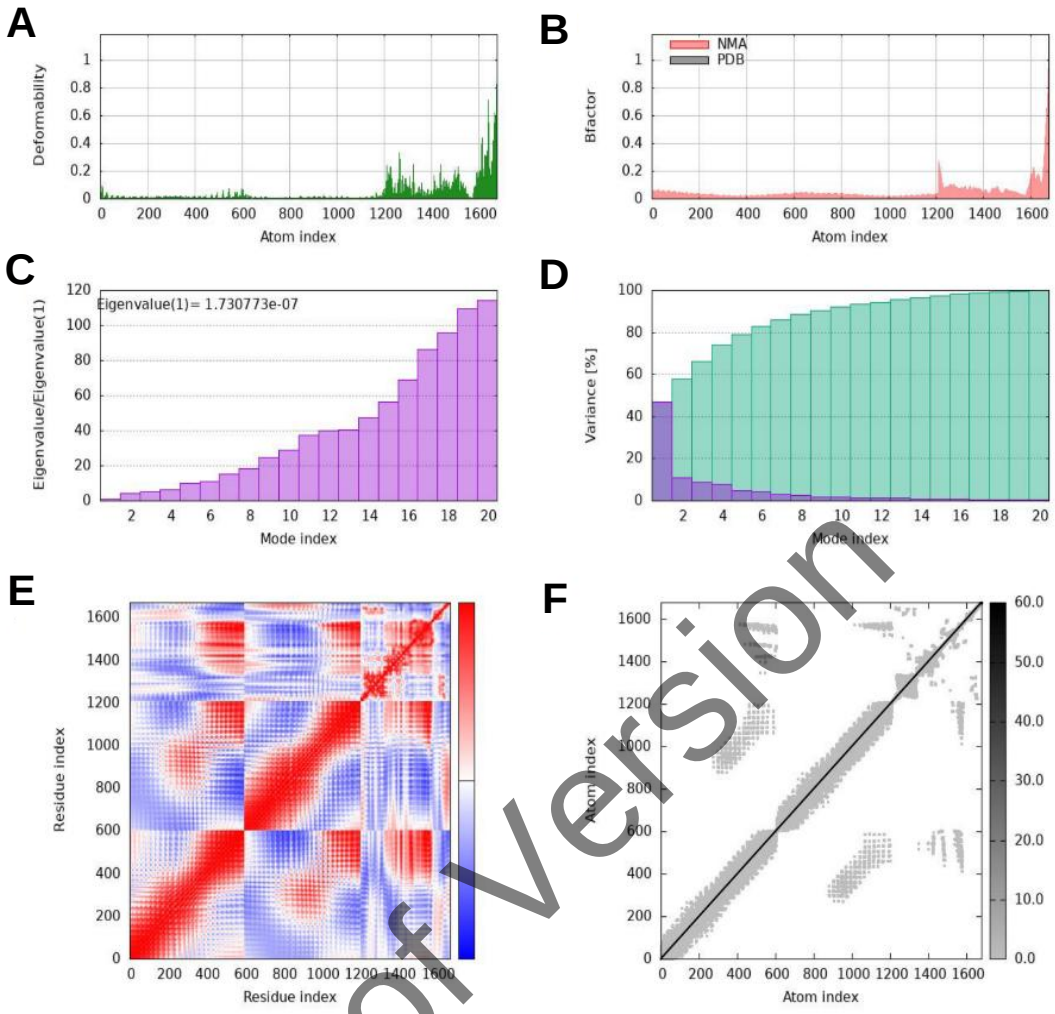
To evaluate the immunogenicity and long-term protective potential of the vaccine construct, a 350-day *in silico* immune simulation—involving a triple-dose administration (days 1, 84, and 168)—was conducted using the C-ImmSim platform. The simulation indicated a theoretically robust primary immune response followed by prominently amplified secondary and tertiary responses, characterized by rapid antigenic clearance and progressive accumulation of high-titer antibodies **(Figure 7A)**. Notably, elevated IgM, IgG1 + IgG2, and total IgG + IgM levels were observed, indicating successful class switching and memory B-cell maturation. The vaccine elicited a potent Th1-polarized cytokine profile, with a marked surge in IFN-γ and IL-2, supplemented by compensatory IL-10 and IL-12 responses **(Figure 7B)**. This cytokine milieu is essential for orchestrating the dual antibacterial and antiviral defense required for HIV–TB control. B-cell population dynamics revealed rapid clonal expansion that peaked and plateaued, suggesting the establishment of durable humoral immunity **(Figure 7C)**. Concurrently, plasma B-cell subsets exhibited consistent growth in IgM + IgG and IgG1 production **(Figure 7D)**.

Analysis of immune-related cellular compartments demonstrated robust production of memory helper (Th) and cytotoxic (Tc) T-cell subsets, critical for long-term surveillance and elimination of intracellular pathogens **(Figure 7E–G)**. Furthermore, the simulation underscored the synergistic activity of innate effector cells, including natural killer cells and macrophages, which reinforced the adaptive response through enhanced phagocytic and cytotoxic functions **(Figure 7H–I)**.

Codon optimization and in silico gene cloning

The construct was cloned into an appropriate expression vector to predict *in silico* expression efficiency. The vaccine was reverse-translated using the Java Codon Adaptation Tool and codon-optimized to obtain a 1,398-base-long nucleotide sequence. It had an average GC content of 54.0%, which was within the recommended range of 30.0%–70.0% for thermodynamic stability. A CAI value of 1 indicated an enhanced probability of efficient prokaryotic expression of the construct. The vaccine was cloned *via* Gibson-PCR assembly **(Figure 8)**, and the optimized sequence was effectively integrated into the pET-30a (+) vector, resulting in a 5,362-bp recombinant construct **(Figure 9)**.

Proof Version



Proof Version

Figure 6. NMA of the vaccine-TLR4 docked complex using the iMODS server. The biophysical stability and inherent flexibility of the complex are illustrated through structural dynamics metrics. **(A)** The Deformability plot, indicating regions of high flexibility (hinges) within the complex, **(B)** The B-factor plot, comparing the theoretical mobility of the complex atoms against experimental normal mode data, **(C)** The Eigenvalue plot, with a computed value of 1.73×10^{-7}, indicating the overall stiffness and energy required to deform the structure, **(D)** The Variance plot, showing the cumulative variance associated with individual normal modes, **(E)** The Covariance matrix, illustrating correlated (red), uncorrelated (white), and anti-correlated (blue) atomic motions, and **(F)** The Elastic Network model, depicting pairs of atoms connected by springs, where darker gray regions represent stiffer spring mechanics. TLR4, toll-like receptor 4.

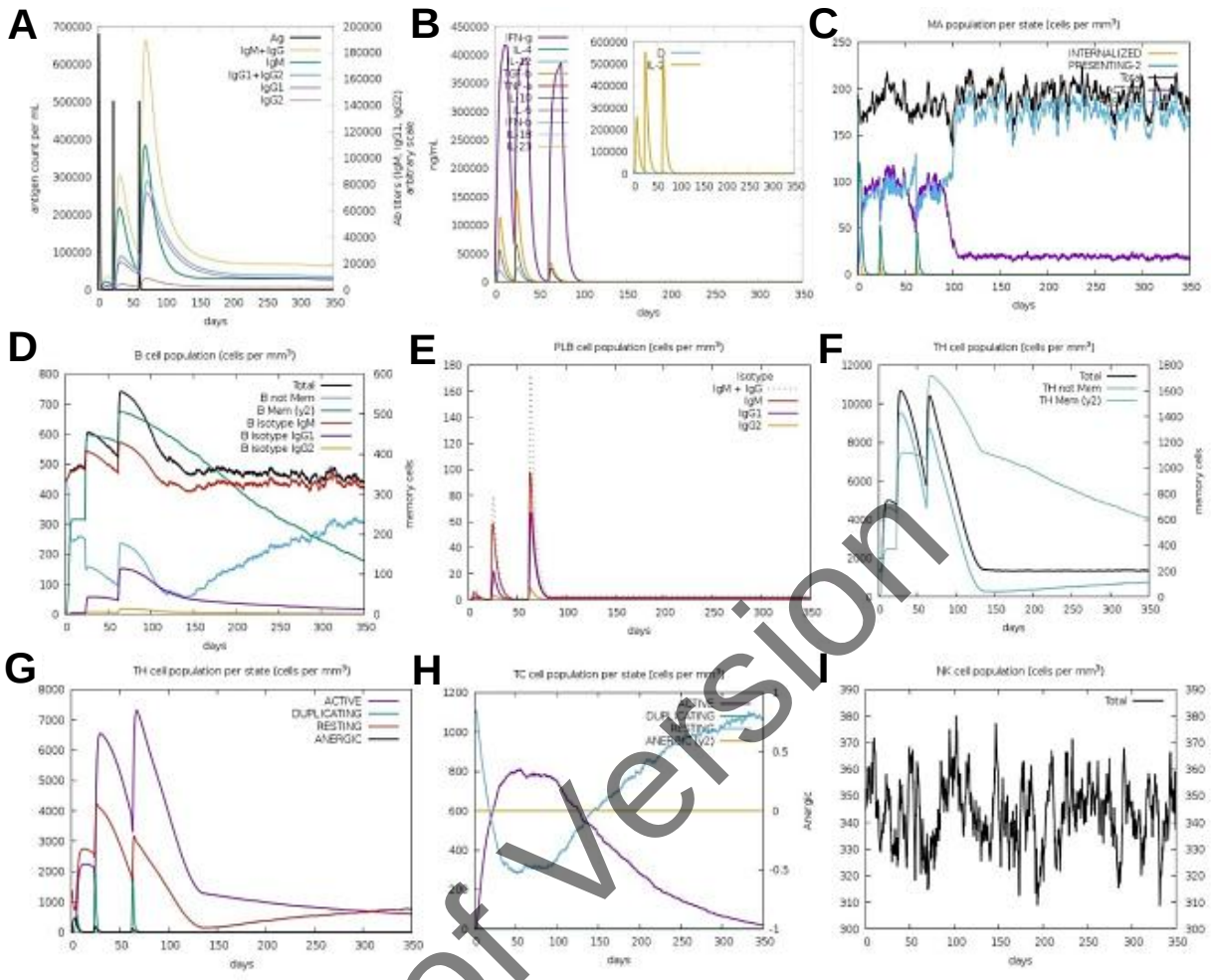
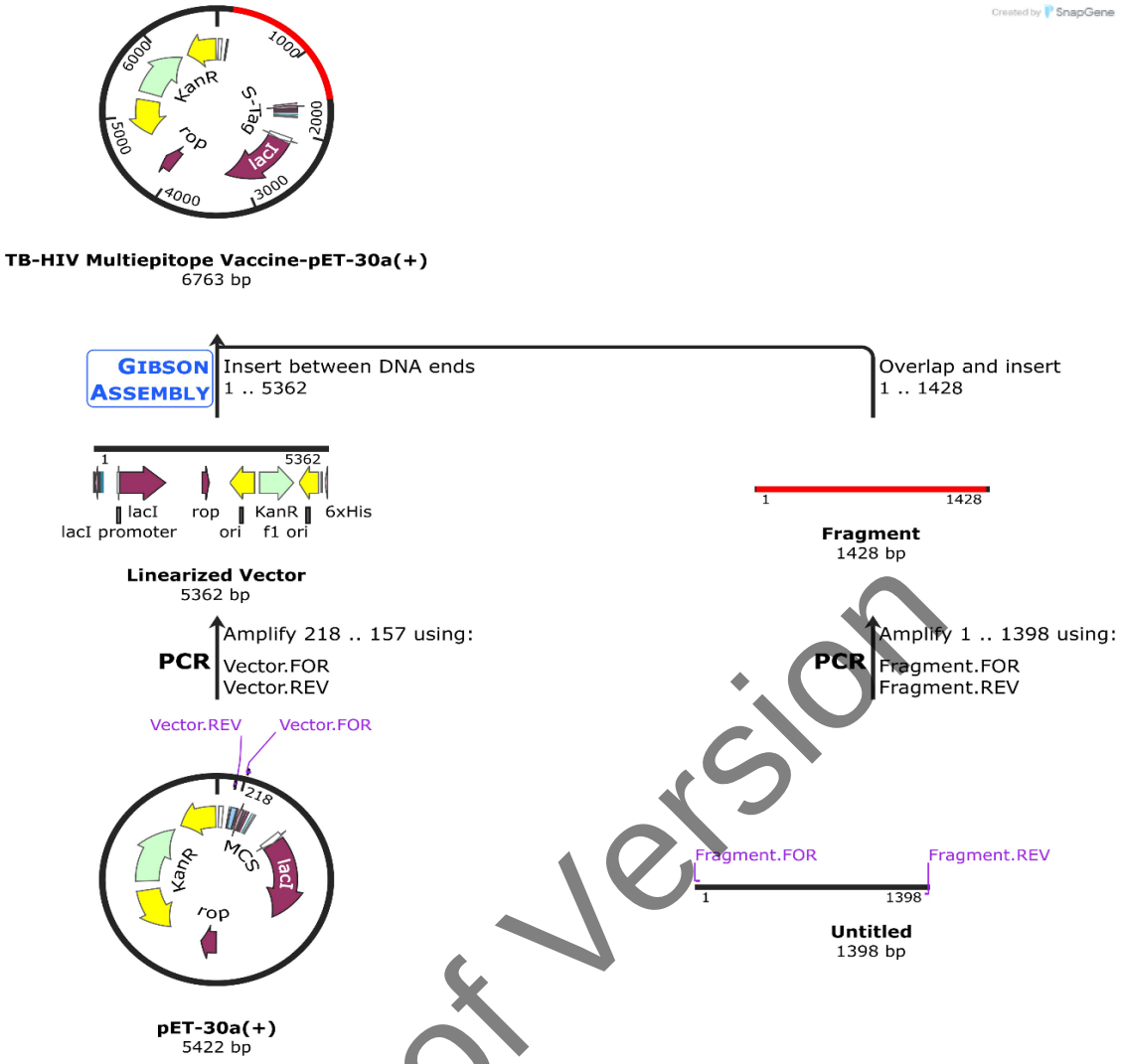


Figure 7. Simulated human immune responses over 350 days following vaccination with the multi-epitope construct. **(A)** Persistent generation of memory antibodies, **(B)** increased expression of cytokines and interleukins, **(C)** enhanced macrophage activity, **(D, E)** expansion of B-cell and plasma B-cell populations, **(F, G)** strengthened helper T-cell responses, **(H)** elevated cytotoxic T-cell activity, and **(I)** augmented natural killer cell responses.

Proof Version



Proof Version

Figure 8. Cloning workflow of the multi-epitope vaccine into the pET-30a (+) vector via Gibson-PCR assembly.

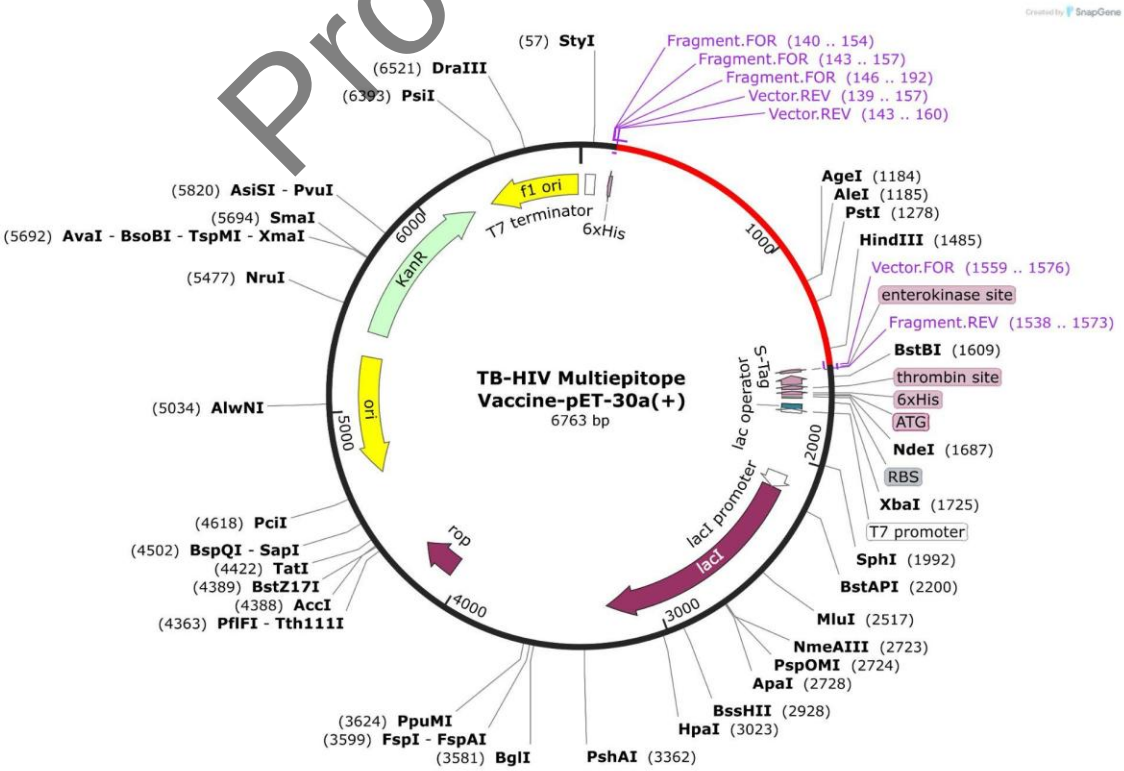
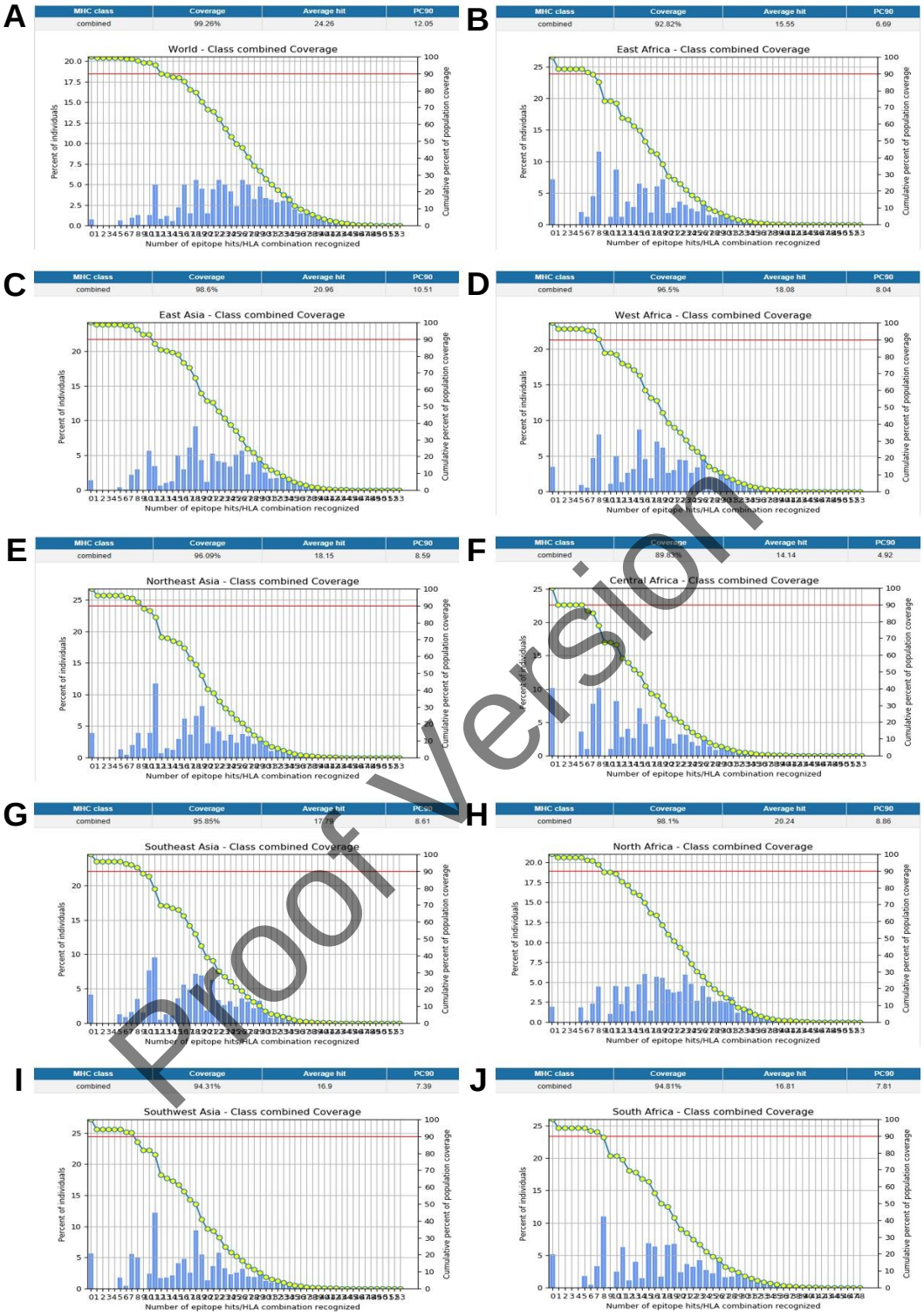


Figure 9. Schematic illustration of the optimized multi-epitope vaccine (red) cloned into the pET-30a (+) expression vector.



Proof Version

Figure 10. Population coverage of the multi-epitope vaccine in **(A)** Global, **(B)** East Africa, **(C)** East Asia, **(D)** West Africa, **(E)** Northeast Asia, **(F)** Central Africa, **(G)** Southeast Asia, **(H)** North Africa, **(I)** Southwest Asia, and **(J)** South Africa population.

Population coverage

HLA allelic distribution differed across geographical regions and ethnic groups worldwide. Therefore, population coverage must be considered while developing an effective vaccine. HLA alleles corresponding to selected CTL and HTL epitopes were collated for population analysis against hotspots. The results demonstrated that the proposed vaccine construct covered 99.26% of HLA alleles presented in the global population **(Figure 10)**.

Discussion

The syndemic interaction between Mtb and HIV represents one of the most significant challenges to global public health, characterized by a lethal synergy that accelerates disease progression and immune exhaustion. [38] HIV-induced depletion of CD4+ T lymphocytes and impaired macrophage activation make individuals ~18 times more likely to progress from latent to active TB. [39,40] In 2023, TB-associated mortality represented nearly one-quarter of all AIDS-related fatalities worldwide. [41] Despite the scale-up of ART, immune reconstitution is often incomplete, leaving HIV-positive patients extremely susceptible to Mtb. Furthermore, the BCG vaccine is strictly contraindicated in symptomatic HIV patients due to a high risk of disseminated BCG disease. [42] In this context, the development of a safe, non-replicating integrated vaccine strategy is a clinical necessity.

Current clinical pipelines largely focus on single-pathogen vaccines. [43] Recent progress in TB vaccines, such as the M72/AS01E subunit vaccine, has shown promise in Mtb-infected adults, [44,45] while such efforts for an HIV vaccine have explored broadly neutralizing antibodies and mRNA platforms (e.g., recent Phase I mRNA-1644 trials). [46] However, a single-pathogen approach fails to address overlapping immune exhaustion within the HIV–TB syndemic. [3] HIV infection actively subverts the granulomatous response required to contain Mtb, whereas Mtb-induced chronic inflammation drives HIV replication. [3,4] By integrating virulence factors from both pathogens—such as Mtb Ag85/ESX-1 and HIV Nef/Vif—we designed a dual-antigen chimeric vaccine to simultaneously disrupt their synergistic immune-evasion strategies, a critical gap in current vaccinology.

Epitopes were selected *via* a rational design strategy to ensure varied and complementary immunological outcomes. High-affinity CTL and HTL epitopes were included to induce a dual-axis immune response. Computational predictions suggest that the selected HTL epitopes can drive a Th1-polarized response, characterized by IFN-γ secretion. Robust IFN-γ production is a key stimulator of macrophage activation and phagolysosome maturation, imperative for intracellular Mtb clearance. [47] Furthermore, the predicted induction of Th2 cytokines (IL-4 and IL-10) theoretically supports B-cell maturation and antibody class switching, vital for neutralizing extracellular HIV virions. [48,49] The balanced activation of Th1/Th2 and regulatory immune pathways can overcome the cell-level immunosuppression observed in co-infected patients.

The CTB subunit was integrated as an N-terminal adjuvant to augment mucosal immunogenicity. The clinical applicability and safety of CTB are well documented; unlike the intact Cholera Toxin, the recombinant B subunit lacks toxicity and is a major component of FDA-approved oral cholera vaccines. [50] Mtb is a respiratory pathogen, and HIV transmission predominantly occurs across mucosal barriers. [51] CTB is extremely effective at breaking mucosal tolerance and bridging innate and adaptive immunity by binding to monosialotetrahexosylganglioside on antigen-presenting cells (APCs). [40,52] Therefore, CTB inclusion theoretically optimizes this construct for mucosal delivery routes (e.g., intranasal), which could establish localized secretory IgA defenses and resident memory T cells at primary sites of pathogen entry, offering an advantage over conventional intramuscular vaccines. [53–55]

Structural viability is a functional prerequisite for this multi-epitope chimera. Secondary structure predictions, indicating a composition dominated by random coils and α-helices, suggest a certain degree of flexibility. This biological feature is favorable, as it facilitates optimal processing and presentation of the embedded epitopes by APCs. [42,56] Furthermore, tertiary structure modeling and validation metrics (such as the ProSA-web Z-score of –3.84) support the hypothesis that the chimeric protein could fold into a stable, native-like conformation without egregious steric clashes, confirming its fundamental biophysical viability before *in vitro* synthesis. [57]

Molecular docking studies predicted a favorable energetic landscape—low thermodynamic energy values—between the vaccine construct and the human TLR4 receptor. [58,59] Furthermore, NMA using iMODS suggested large-scale molecular mobility and inherent elasticity of the complex, indicating that the predicted binding pose requires minimal conformational entropy to remain stable. [60] However, these computational outputs represent thermodynamic probabilities, not definitive proof of bioefficacy or *in vivo* receptor activation. While NMA provides valuable insights into macromolecular rigidity and induced-fit potential, it is a coarse-grained simulation. [61]

Similarly, *in silico* immune simulations predicting rapid antigen clearance and memory cell expansion serve exclusively as hypothesis-generating data. While these algorithms are built on validated empirical immunological datasets, they cannot fully capture the extreme complexity of HIV-associated immune exhaustion, spatial dynamics of Mtb granulomas, or

Proof Version

population-specific HLA polymorphisms. Therefore, all findings regarding immune activation, structural stability, and clinical suitability presented herein remain strict theoretical constructs.

This study is limited by its *in silico* design; therefore, predicted immunogenicity, safety, and durability of immune responses require experimental validation. Computational models may not fully capture the complexity of HIV-associated immune dysfunction and latent Mtb infection nor account for population-specific HLA variability. The current pipeline did not benchmark the immune simulation outputs against a comparative control construct. Additionally, the adjuvant performance of the CTB subunit in a dual-pathogen vaccine context remains to be empirically confirmed. Future studies should prioritize *in vitro* and *in vivo* validation, including immunogenicity and challenge models relevant to HIV–TB co-infection to ensure vaccine safety, immunogenicity, and effectiveness.

Conclusion

This study rationally designed a novel chimeric multi-epitope vaccine targeting the synergistic pathogenesis of HIV–TB co-infection. Using a comprehensive immunoinformatics pipeline, we integrated literature-validated essential virulence factors into a single construct that suggests a favorable theoretical binding affinity to the TLR4 receptor and structural stability during NMA. Furthermore, it was predicted to induce a balanced Th1/Th2 immune response. While the projected global and regional population coverage was notably high, these computational predictions are inherently limited by HLA allelic diversity modeling and the absence of complex biological parameters. Therefore, this chimeric construct provides a robust theoretical foundation that requires future *in vitro* and *in vivo* experimental validation to establish its clinical safety and immunogenic efficacy.

Authors contributions

NA and MIA contributed substantially to the concept and design of this study, literature review, and acquiring, analyzing, and interpreting data. SYA, IMF, ILE, PAA, MAHK, MAA, and MCAA contributed substantially to acquiring data and manuscript drafting. AMR and APS edited the manuscript critically for intellectual content. All authors approved the final submitted version and assume responsibility for statements made.

Acknowledgments

Not applicable

Funding

The authors received no funding for this project.

Conflict of interest statement

The authors declare no competing interests.

Data sharing statement

All data generated or analyzed during the present study are included in this published article. Further details are available for non-commercial purposes from the corresponding author on reasonable request.

AI declaration

Generative AI tools were utilized to support the preparation of this manuscript. Grammarly and Gemini AI were used to help refine wording, improve clarity, and correct grammar and spelling. All content was critically reviewed and edited by the authors to ensure accuracy, originality, and adherence to ethical standards.

ORCID

Nabil Athoillah https://orcid.org/0000-0002-2678-9535
Muhammad Irsyad Amien https://orcid.org/0000-0002-5672-6957
Saski Yasmin Alfina https://orcid.org/0009-0007-8173-0871
Ichlasul Mahdi Fardhani https://orcid.org/0000-0003-1538-3318
Irsyad Lutfi Elfahmi https://orcid.org/0009-0005-3966-1070
Putri Ayu Ardiani https://orcid.org/0009-0006-6176-0478
Mukhammad Arif Hadi Khoiruddin https://orcid.org/0000-0001-6559-803X
Mohammad Alifi Agfareza https://orcid.org/0009-0004-3815-917X
Mitsla Chusnica Aulia As'ar https://orcid.org/0009-0009-6233-6072
Angga Mardro Raharjo https://orcid.org/0000-0001-5533-1438
Atika Purnama Sari https://orcid.org/0009-0002-0249-6903

References

1. Feng L, Wang Y, Li L, Wang X, Feng J. Global burden of HIV and drug-resistant tuberculosis co-infection and its attributable risk factors, 1990 to 2021, with projections to 2031. BMC Infect Dis 2025;25:1521.

Proof Version

2. Ignatious EH, Swindells S. Update on tuberculosis/HIV coinfections: across the spectrum from latent infection through drug-susceptible and drug-resistant disease. Top Antivir Med 2022;30:464–72.
3. Gunawan CK, Sumarpo A, Indrati AR. Immune Dysregulation in HIV-TB Co-Infection: Role of Cytokines and T Cell Biomarkers—A Narrative Review. Pathogens 2026;15:51.
4. Sharan R, Bucşan AN, Ganatra S, Paiardini M, Mohan M, Mehra S, et al. Chronic Immune Activation in TB/HIV Co-infection. Trends Microbiol 2020;28:619–32.
5. Sossen B, Kubjane M, Meintjes G. Tuberculosis and HIV coinfection: Progress and challenges towards reducing incidence and mortality. Int J Infect Dis 2025;155:107876.
6. Patel A, Pundkar A, Agarwal A, Gadkari C, Nagpal AK, Kuttan N. A comprehensive review of hiv-associated tuberculosis: clinical challenges and advances in management. Cureus 2024;16:68784.
7. Mase SR, Chorba T. Treatment of drug-resistant tuberculosis. Clin Chest Med 2019;40:775–95.
8. Nagpal G, Usmani SS, Raghava GPS. A Web Resource for Designing subunit vaccine against major pathogenic species of bacteria. Front Immunol 2018;9:2280.
9. Albutti A. An integrated computational framework to design a multi-epitopes vaccine against Mycobacterium tuberculosis. Sci Rep 2021;11:21929.
10. Ismail S, Alsowayeh N, Abbasi HW, et al. Pan-Genome-Assisted Computational Design of a Multi-Epitopes-Based Vaccine Candidate against Helicobacter cinaedi. Int J Environ Res Public Health 2022;19:11579.
11. Srivastava S, Verma S, Kamthania M, Kaur R, Badyal RK, Saxena AK, et al. Structural Basis for Designing Multiepitope Vaccines Against COVID-19 Infection: In Silico Vaccine Design and Validation. JMIR Bioinform Biotechnol 2020;1:19371.
12. Azim KF, Hasan M, Hossain MN, Somana SR, Hoque SF, Bappy MNI, et al. Immunoinformatics approaches for designing a novel multi epitope peptide vaccine against human norovirus (Norwalk virus). Infect Genet Evol 2019;74:103936.
13. Liu B, Zheng D, Jin Q, Chen L, Yang J. VFDB 2019: a comparative pathogenomic platform with an interactive web interface. Nucleic Acids Res 2019;47 D1:687–92.
14. Shukla M, Wattam AR, Aleman A, Bhattacharya R, Bowers N, Brettin T, et al. BV-BRC: a unified bacterial and viral bioinformatics resource with expanded functionality and AI integration. Nucleic Acids Res 2026;54:715–23.
15. Negi SS, Braun W. Cross-React: a new structural bioinformatics method for predicting allergen cross-reactivity. Bioinformatics 2017;33:1014–20.
16. Karbalaei Zadeh Babaki M, Soleimanpour S, Rezaee SA. Antigen 85 complex as a powerful Mycobacterium tuberculosis immunogene: Biology, immune-pathogenicity, applications in diagnosis, and vaccine design. Microb Pathog 2017;112:20–9.
17. Ramon-Luing L, Palacios Y, Ruiz A, Téllez-Navarrete N, Chavez-Galan L. Virulence Factors of Mycobacterium tuberculosis as Modulators of Cell Death Mechanisms. Pathogens 2023;12:839.
18. Fettig J, Swaminathan M, Murrill CS, Kaplan JE. Global epidemiology of HIV. Infect Dis Clin North Am 2014;28:323–37.
19. Fleri W, Paul S, Dhanda SK, Mahajan S, Xu X, Peters B, et al. The Immune epitope database and analysis resource in epitope discovery and synthetic vaccine design. *Front* Immunol 2017;8:278.
20. Doytchinova IA, Flower DR. VaxiJen: a server for prediction of protective antigens, tumour antigens and subunit vaccines. BMC Bioinformatics 2007;8:4.
21. Dimitrov I, Bangov I, Flower DR, Doytchinova I. AllerTOP v.2—a server for in silico prediction of allergens. J Mol Model 2014;20:2278.
22. Gupta S, Kapoor P, Chaudhary K, Gautam A, Kumar R. In silico approach for predicting toxicity of peptides and proteins. PLoS One 2013;8:e73957.
23. Ali M, Pandey RK, Khatoon N, Narula A, Mishra A, Prajapati VK. Exploring dengue genome to construct a multi-epitope based subunit vaccine by utilizing immunoinformatics approach to battle against dengue infection. Sci Rep 2017;7:9232.
24. Nagpal G, Usmani SS, Dhanda SK, et al. Computer-aided designing of immunosuppressive peptides based on IL-10 inducing potential. Sci Rep 2017;7:42851.
25. Ashayeripanah M. Screening and in silico evaluation of candidate late-stage antigens for incorporation into multi-stage and post-exposure vaccines against tuberculosis. NPJ vaccines 2026;11:72.
26. Rahimi-Farsi N, Bostanian F, Ahmadi K, Zangooie A, Sedighi M, Shahbazi B, et al. Immunoinformatic-driven design of a multi-epitope vaccine against Helicobacter pylori. Biochem Biophys Reports 2026;45:102498.
27. Zhang M, Ali SL, Tian Y, Abduldayeva A, Zhou S, An Y, et al. EP9158H: An Immunoinformatics-Designed mRNA Vaccine Encoding Multi-Epitope Antigens and Dual TLR Agonists for Tuberculosis Prevention. Bioengineering 2025;12:1378.
28. Roy S, Maheshwari N, Chauhan R, Sen NK, Sharma A. Structure prediction and functional characterization of secondary metabolite proteins of Ocimum. Bioinformation 2011;6:315–9.
29. Buchan DWA, Jones DT. The PSIPRED protein analysis workbench: 20 years on. Nucleic Acids Res 2019;47:402–7.
30. Jumper J, Evans R, Pritzel A, et al. Highly accurate protein structure prediction with AlphaFold. Nature 2021;596:583–9.
31. Heo L, Park H, Seok C. GalaxyRefine: protein structure refinement driven by side-chain repacking. Nucleic Acids Res 2013;41:384–8.
32. Wiederstein M, Sippl MJ. ProSA-web: interactive web service for the recognition of errors in three-dimensional structures of proteins. Nucleic Acids Res 2007;35(Web Server issue):W407–10.

Proof Version

33. Oladejo DO, Oduselu GO, Dokunmu TM, Isewon I, Oyelade J, Okafor E, et al. In silico Structure Prediction, Molecular Docking, and Dynamic Simulation of Plasmodium falciparum AP2-I Transcription Factor. Bioinform Biol Insights 2023;17:11779322221149616.
34. Kozakov D, Hall DR, Xia B, Porter KA, Padhorny D, Yueh C, et al. The ClusPro web server for protein-protein docking. Nat Protoc 2017;12:255–78.
35. López-Blanco JR, Aliaga JI, Quintana-Ortí ES, Chacón P. iMODS: internal coordinates normal mode analysis server. Nucleic Acids Res 2014;42:271–6.
36. Rapin N, Lund O, Bernaschi M, Castiglione F. Computational immunology meets bioinformatics: the use of prediction tools for molecular binding in the simulation of the immune system. PLoS One 2010;5:9862.
37. Goller CC, Srougi MC, Chen SH, Schenkman LR, Kelly RM. Integrating bioinformatics tools into inquiry-based molecular biology laboratory education modules. Front Educ 2021;6:711403.
38. Waters R, Ndengane M, Abrahams MR, Diedrich CR, Wilkinson RJ, Coussens AK. The Mtb -HIV Syndemic Interaction: Why Treating M. tuberculosis Infection May Be Crucial for HIV-1 Eradication. Future Virol 2020;15:101-26.
39. Rcheulishvili N, Mao J, Papukashvili D, et al. Design, evaluation, and immune simulation of potentially universal multi-epitope mpox vaccine candidate: focus on DNA vaccine. Front Microbiol 2023;14:1203355.
40. Stratmann T. Cholera toxin subunit b as adjuvant—an accelerator in protective immunity and a break in autoimmunity. Vaccines 2015;3:579–96.
41. Souod N, Madanchi H, Bahrami F, Pakzad SR, Shahcheraghi F, Ajdary S. In silico design and evaluation of a multiepitope vaccine against Bordetella pertussis: structural, immunological, and biological properties. Genomics Inform 2025;23:16.
42. Elrashedy A, Nayel M, Salama A, Salama MM, Hasan ME. Bioinformatics approach for structure modeling, vaccine design, and molecular docking of Brucella candidate proteins BvrR, OMP25, and OMP31. Sci Rep 2024;14:11951.
43. He Y, Xie X, He S, Li S, Zhou H, Wei S. Immunotherapy for tuberculosis: current landscape, mechanistic insights, and translational perspectives. Front Immunol 2026;17:1859046.
44. Tait DR, Hatherill M, Van Der Meeren O, et al. Final Analysis of a Trial of M72/AS01 E Vaccine to Prevent Tuberculosis. N Engl J Med 2019;381:2429–39.
45. Maani A Al, Petersen E, Memish ZA. The critical role of new tuberculosis vaccines in achieving the WHO 2035 End TB target. IJID Reg 2025;14:100595.
46. Fortner A, Bucur O. mRNA-based vaccine technology for HIV. Discov (Craiova) 2022;10:150.
47. Imran M, Alshrari AS, Khan A, Alzahrani AR. IFN-γ-Driven macrophage responses in the immunity to Mycobacterium tuberculosis and Mycobacterium leprae. Front Cell Infect Microbiol 2025;15:1679691.
48. Burton DR, Hangartner L. Broadly Neutralizing Antibodies to HIV and Their Role in Vaccine Design. Annu Rev Immunol 2016;34:635–59.
49. Wang R, Lan C, Benlagha K, Camara NOS, Miller H, Kubo M, et al. The interaction of innate immune and adaptive immune system. MedComm 2024;5:714.
50. Baldauf KJ, Royal JM, Hamorsky KT, Matoba N. Cholera toxin B: one subunit with many pharmaceutical applications. Toxins (Basel) 2015;7:974–96.
51. Neutra MR, Kozlowski PA. Mucosal vaccines: the promise and the challenge. Nat Rev Immunol 2006;6:148–58.
52. Holmgren J, Czerkinsky C, Eriksson K, Mharandi A. Mucosal immunisation and adjuvants: a brief overview of recent advances and challenges. Vaccine 2003;21: S89–S95.
53. Hou J, Liu Y, Hsi J, Wang H, Tao R, Shao Y. Cholera toxin B subunit acts as a potent systemic adjuvant for HIV-1 DNA vaccination intramuscularly in mice. Hum Vaccin Immunother 2014;10:1274–83.
54. Park SC, Wiest MJ, Yan V, Wong PT, Schotsaert M. Induction of protective immune responses at respiratory mucosal sites. Hum Vaccin Immunother 2024;20:2368288.
55. Kwon DI, Bhagchandani SH, Ehrenzeller SA, Iwasaki A. Harnessing mucosal immunity for protective vaccines. Nat Rev Immunol 2026;26:507–24.
56. Yakimov AP, Afanaseva AS, Khodorkovskiy MA, Petukhov MG. Design of Stable α-Helical Peptides and Thermostable Proteins in Biotechnology and Biomedicine. Acta Naturae 2016;8:70–81.
57. Akter NN, Uddin MM, Uddin N, Asha IJ, Uddin MS, Hossain MA, et al. Structural and functional characterization of a putative type vi secretion system protein in cronobacter sakazakii as a potential therapeutic target: a computational study. Evol Bioinform Online 2025;21:11769343251327660.
58. Kozakov D, Hall DR, Xia B, Porter KA, Padhorny D, Yueh C, et al. The ClusPro web server for protein–protein docking. Nat Protoc 2017;12:255–78.
59. Ismail S, Abbasi SW, Yousaf M, Ahmad S, Muhammad K, Waheed Y. Design of a multi-epitopes vaccine against hantaviruses: an immunoinformatics and molecular modelling approach. Vaccines 2022;10:378.
60. Sami SA, Marma KKS, Mahmud S, Khan MAN, Albogami S, El-Shehawi AM, et al. Designing of a Multi-epitope Vaccine against the Structural Proteins of Marburg Virus Exploiting the Immunoinformatics Approach. ACS Omega 2021;6:32043–71.
61. Meireles L, Gur M, Bakan A, Bahar I. Pre-existing soft modes of motion uniquely defined by native contact topology facilitate ligand binding to proteins. Protein Sci 2011;20:1645–58.

Proof Version